Chronic Meningitis Investigated via Metagenomic Next-Generation Sequencing

Michael R. Wilson, MD, MAS; Brian D. O'Donovan, MS; Jeffrey M. Gelfand, MD, MAS; Hannah A. Sample, BS; Felicia C. Chow, MD, MAS; John P. Betjemann, MD; Maulik P. Shah, MD; Megan B. Richie, MD; Mark P. Gorman, MD; Rula A. Hajj-Ali, MD; Leonard H. Calabrese, DO; Kelsey C. Zorn, MHS; Eric D. Chow, PhD; John E. Greenlee, MD; Jonathan H. Blum, MD, PhD; Gary Green, MD; Lillian M. Khan, BS; Debarko Banerji, BS; Charles Langelier, MD, PhD; Chloe Bryson-Cahn, MD; Whitney Harrington, MD, PhD; Jairam R. Lingappa, MD, PhD; Niraj M. Shanbhag, MD, PhD; Ari J. Green, MD, MAS; Bruce J. Brew, MBBS, DMedSci, DSc; Ariane Soldatos, MD; Luke Strnad, MD; Sarah B. Doernberg, MD, MAS; Cheryl A. Jay, MD; Vanja Douglas, MD; S. Andrew Josephson, MD; Joseph L. DeRisi, PhD

IMPORTANCE Identifying infectious causes of subacute or chronic meningitis can be challenging. Enhanced, unbiased diagnostic approaches are needed.

OBJECTIVE To present a case series of patients with diagnostically challenging subacute or chronic meningitis using metagenomic next-generation sequencing (mNGS) of cerebrospinal fluid (CSF) supported by a statistical framework generated from mNGS of control samples from the environment and from patients who were noninfectious.

DESIGN, SETTING, AND PARTICIPANTS In this case series, mNGS data obtained from the CSF of 94 patients with noninfectious neuroinflammatory disorders and from 24 water and reagent control samples were used to develop and implement a weighted scoring metric based on z scores at the species and genus levels for both nucleotide and protein alignments to prioritize and rank the mNGS results. Total RNA was extracted for mNGS from the CSF of 7 participants with subacute or chronic meningitis who were recruited between September 2013 and March 2017 as part of a multicenter study of mNGS pathogen discovery among patients with suspected neuroinflammatory conditions. The neurologic infections identified by mNGS in these 7 participants represented a diverse array of pathogens. The patients were referred from the University of California, San Francisco Medical Center (n = 2), Zuckerberg San Francisco General Hospital and Trauma Center (n = 2), Cleveland Clinic (n = 1), University of Washington (n = 1), and Kaiser Permanente (n = 1). A weighted z score was used to filter out environmental contaminants and facilitate efficient data triage and analysis.

MAIN OUTCOMES AND MEASURES Pathogens identified by mNGS and the ability of a statistical model to prioritize, rank, and simplify mNGS results.

RESULTS The 7 participants ranged in age from 10 to 55 years, and 3 (43%) were female. A parasitic worm (*Taenia solium*, in 2 participants), a virus (HIV-1), and 4 fungi (*Cryptococcus neoformans*, *Aspergillus oryzae*, *Histoplasma capsulatum*, and *Candida dubliniensis*) were identified among the 7 participants by using mNGS. Evaluating mNGS data with a weighted z score–based scoring algorithm reduced the reported microbial taxa by a mean of 87% (range, 41%-99%) when taxa with a combined score of 0 or less were removed, effectively separating bona fide pathogen sequences from spurious environmental sequences so that, in each case, the causative pathogen was found within the top 2 scoring microbes identified using the algorithm.

CONCLUSIONS AND RELEVANCE Diverse microbial pathogens were identified by mNGS in the CSF of patients with diagnostically challenging subacute or chronic meningitis, including a case of subarachnoid neurocysticercosis that defied diagnosis for 1 year, the first reported case of CNS vasculitis caused by *Aspergillus oryzae*, and the fourth reported case of *C dubliniensis* meningitis. Prioritizing metagenomic data with a scoring algorithm greatly clarified data interpretation and highlighted the problem of attributing biological significance to organisms present in control samples used for metagenomic sequencing studies.

← Editorial

+ Supplemental content

Author Affiliations: Author affiliations are listed at the end of this article.

Corresponding Author: Michael R. Wilson, MD, MAS, Department of Neurology, UCSF Weill Institute for Neurosciences, 675 Nelson Rising Ln, NS212A, Campus Box 3206, San Francisco, CA 94158 (michael.wilson@ucsf.edu).

Subacute and chronic meningitis are diagnostically challenging given the wide range of potential infectious, autoimmune, neoplastic, paraneoplastic, parameningeal, and toxic causes.[1,2] Securing a final diagnosis can require weeks or months of testing or remain unsolved, necessitating empirical treatment approaches that may be ineffective or even harmful.

Unlike traditional testing for specific microbes or categories of infection, metagenomic next-generation sequencing (mNGS) of cerebrospinal fluid (CSF) or brain tissue screens for nearly all potential central nervous system (CNS) infections and can identify novel or unexpected pathogens.[3-10] Multiple computational algorithms and pipelines have been developed to rapidly identify microbial sequences in mNGS data sets.[11-13] However, mNGS data require careful analysis to determine which, if any, of the identified microbes represent a true pathogen rather than environmental contamination. Failure to make this distinction has resulted in spurious disease associations with organisms later determined to be laboratory contaminants.[14-16]

In the present study, we developed a straightforward statistical approach to analyze mNGS data, leveraging an extensive mNGS database of water-only control samples (n = 24) and surplus CSF samples (n = 94) obtained from patients with clinically adjudicated noninfectious neurologic diagnoses, including autoimmune, neoplastic, structural, and neurodegenerative disorders (a control cohort). This statistical approach quantified the uniqueness of observing a particular microbe in a patient sample at a given level of abundance by comparison with its mean level of abundance across the control cohort. We report herein the utility of this statistical framework for identifying microbial pathogens in 7 challenging cases of subacute or chronic meningitis as well as for analyzing publicly available data from recent mNGS infectious diagnostic and brain microbiota studies.[17-19]

Methods

Participants were recruited between September 2013 and March 2017 as part of a larger study applying mNGS to biological samples from patients with suspected neuroinflammatory disease. The 7 participants enrolled in the present study had subacute or chronic leptomeningitis with or without encephalitis. An etiologic diagnosis was not known by the researchers at the time of study enrollment. If a diagnosis was made by traditional means before mNGS testing was completed (participants 3, 5, and 6), the researchers performing mNGS (M.R.W. and J.L.D.) remained blinded to the diagnosis. The patients were referred from the UCSF (University of California, San Francisco) Medical Center (n = 2), Zuckerberg San Francisco General Hospital (n = 2), Cleveland Clinic (n = 1), University of Washington (n = 1), and Kaiser Permanente (n = 1). The UCSF Institutional Review Board approved the study protocol, and participants or their surrogates provided written informed consent. Treating physicians were informed about research-based mNGS results through a reporting mechanism approved by the UCSF Institutional Review Board.

Key Points

Question How can metagenomic next-generation sequencing of cerebrospinal fluid be leveraged to aid in the diagnosis of patients with subacute or chronic meningitis?

Findings In this case series, metagenomic next-generation sequencing identified a parasitic worm, a virus, and 4 fungi among 7 participants with subacute or chronic meningitis. A database generated using water-only and healthy patient control samples enabled application of a z score–based scoring algorithm to effectively separate bona fide pathogen sequences from spurious environmental sequences.

Meaning The scoring algorithm greatly simplified data interpretation among patients with a wide range of challenging infectious causes of subacute or chronic meningitis identified by metagenomic next-generation sequencing.

mNGS Protocol

Metagenomic next-generation sequencing was performed on total RNA extracted from surplus CSF (250-500 μL), and 1 participant also had mNGS performed on total RNA extracted from snap frozen surplus tissue (<50 mg) obtained from a lumbar meningeal biopsy. Samples were processed for mNGS as previously described.[5,7] The nonhuman sequence reads from each sample were deposited at the National Center for Biotechnology Information Sequence Read Archive (PRJNA338853).

Bioinformatics Analysis

Paired-end sequences of 125 to 150 base pairs were analyzed using a previously described rapid computational pathogen detection pipeline consisting of open-source components (**Figure 1**).[5,7,20-26] Unique nonhuman sequences were assigned to microbial taxonomic identifiers based on nucleotide (nt) and nonredundant (nr) protein alignments. To distinguish putative pathogens from contaminating microbial sequences derived from skin, collection tubes, laboratory reagents, or the environment, a composite background model of metagenomic data was used. This model incorporated 24 water control samples and 94 CSF samples from patients with noninfectious diagnoses, including 21 patients with chronic meningitis with or without encephalitis. Data were normalized to unique reads mapped per million (RPM) input reads for each microbe at the species and genus level.

Statistical Analysis

Using the aforementioned background data set as the expected mean RPM for a given taxonomic identifier, standard z scores were calculated for each genus (gs) and species (sp) in each sample based on the results from both the nt and nr database searches. Thus, there are 4 z scores reported for each sample: spznt, gsznt, spznr, and gsznr. To prioritize reporting of the most unique (ie, unexpected) taxa in each sample, the significance of each microbial species was mapped to a single value with the following empirically derived formula: score = spznt (gsznt [RPM − nt]) + spznr (gsznr [RPM − nr]).

Here, RPM is scaled by the z scores for both the species and the genus. If both z scores were negative, the product remained negative. The maximum z score was arbitrarily capped

Figure 1. Computational Pathogen Detection Pipeline

	Read-pairs, No.	Retained, %	Time, min	Component	Target
Raw sequence, .fastq files	13 141 550	100	0.0	NA	NA
First pass removal of human reads	1 930 493	14.7	7.2	STAR	Hg38/PanTro4 RepBase
Quality filter	538 661	4.1	7.9	PriceSeqFilter	Read-pairs
Compression of redundant reads	374 592	2.8	8.1	CD-HIT-DUP	Read-pairs
LZW complexity filter	347 719	2.6	9.5	LZW (script)	Read-pairs
Second pass paired-end human read removal	63 435	0.5	10.9	Bowtie 2	Hg38/RepBase
Alignment to nt database	62 855	0.5	12.3	GMAP/GSNAP	NCBI nt
Alignment to nr database	62 514	0.5	19.5	RAPSearch2	NCBI nr
Taxonomic statistics/reporting	58 789	94.0 of Nonhost	19.6	PHP/MySQL	NCBI taxonomy

→ Aligns to Genus *Taenia*

A rapid computational pipeline was implemented as diagrammed for detection of potential pathogen-derived sequences. Values for participant 1 are shown as an example. The cerebrospinal fluid sample obtained from participant 1 yielded 13 141 550 million read-pairs, which were then subjected to removal of human reads by spliced transcripts alignment to a reference (STAR, version 2.4.2),[20] quality control filtering (PriceSeqFilter, version 1.1.2),[21] compression of duplicate reads (CD-HIT-DUP, version 4.6.4-2015),[22] removal of low-complexity sequences by filtering for high Lempel-Ziv-Welch (LZW)[23] compression ratios, a second round of removal of human reads (Bowtie 2, version 2.2.4),[24] alignment to the National Center for Biotechnology Information (NCBI) nucleotide (nt) database (GMAP/GSNAP, version 2015-12),[25] alignment to the NCBI nonredundant (nr) protein database (RAPSearch2, version 2.23),[26] and statistical calculation and taxonomy reporting using PHP/MySQL, version 5.5.53. The entire computational pipeline was completed in 19.6 min using a single high-end server (32 core, Intel Xeon E5-2667 v3 with a 3.2-GHz processor and 768 Gb of RAM). NA indicates not applicable.

at 100. This product was calculated for alignments to both the nt and nr databases and summed. The top-ranked taxa were considered with respect to the clinical features of the participant. Microbes with known CNS pathogenicity that could cause a clinical phenotype concordant with the clinical presentation were considered potential pathogens and were confirmed using standard microbiologic assays, as described in the brief case histories presented below.

Results

The age of the 7 study participants ranged from 10 to 55 years, and 3 participants (43%) were female. Additional clinical characteristics are given in **Table 1**. In each case, the causative pathogen was found within the top 2 scoring microbes identified by our algorithm (**Figure 2**). Across the 7 study participants, the mean of the reported taxa was reduced by 87% (range, 41%-99%) when taxa with a combined score of zero or less were removed (mean before filtering: 307 [range, 11-1313] taxa; after filtering: 53 [range 1-297 taxa]).

Case Descriptions

Taenia solium

Participant 1 was a 28-year-old man from Central America with headache and diplopia. An examination of his CSF revealed an opening pressure greater than 50 cm, white blood cell (WBC) count of 66 000/μL (to convert to ×10⁹ per liter, multiply by 0.001) comprising 89% lymphocytes, 4% neutrophils, 4% monocytes, and 3% eosinophils (to convert to a proportion, multiply by 0.01), red blood cell (RBC) count of 1×10^6/μL (to convert to ×10¹² per liter, multiply by 1), total protein level of 43 mg/dL (reference range, 15-50 mg/dL; to convert to grams per liter, multiply by 0.01), and glucose level of 27 mg/dL (reference range, 40-70 mg/dL; to convert to millimoles per liter, multiply by 0.0555). Contrast-enhanced brain magnetic resonance imaging (MRI) revealed enhancement of the basilar meninges and several cranial nerves (**Figure 3**A). Although the serum cysticercosis antibody test result was positive, there were no cysts or calcifications detected on brain MRI. The low CSF glucose level, basilar meningitis, positive tuberculin skin test, positive tuberculosis interferon-gamma release assay, and high-risk region of origin prompted empirical treatment of

Table 1. Clinical Characteristics of the 7 Participants

Participant No./Sex/Age, y	Final Diagnosis	Clinical Presentation	Disease Duration at Time of Diagnostic LP, mo	Length of Follow-up, mo
1/M/28	*Taenia solium*	Headache, diplopia	11	8
2/F/34	*T solium*	Headache, unilateral facial numbness and tinnitus, recurrent loss of consciousness	9	21
3/M/52	*Cryptococcus neoformans*	Seizures, coma	3	19
4/M/55	HIV-1	Dementia, cough, night sweats, weight loss	0.5	7
5/M/32	*Aspergillus oryzae*	Headache, dizziness, diplopia, unilateral facial weakness and numbness	7	1
6/F/10	*Histoplasma capsulatum*	Back pain followed by unilateral facial droop, headache, neck stiffness	6	3.5
7/F/26	*Candida dubliniensis*	Low back pain followed by saddle anesthesia and unilateral foot drop	20	1

Abbreviations: F, female; LP, lumbar puncture; M, male.

Figure 2. Ranked Results of Statistical Scoring
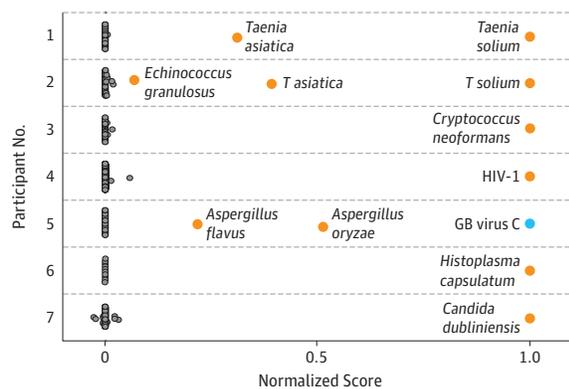
Strip plot of normalized species significance scores for microbial taxa (colored circles) in each participant sample (row). In 6 of 7 samples, the neurologic infection (orange circles) is ranked as the most significant by our approach. In participant number 5, *Aspergillus oryzae* is ranked second behind GB virus C, a likely concurrent infection unassociated with the clinical presentation (blue circle). Microbes likely representing environmental contaminants are also shown (gray circles).

Mycobacterium tuberculosis (TB) meningitis. The patient improved clinically during the next 3 weeks but then worsened, requiring multiple lumbar punctures (LPs), MRIs, and hospitalizations during the next year. Subsequent CSF samples showed worsening lymphocytic pleocytosis and persistently low glucose and elevated protein levels. Neuroimaging results showed persistent basilar meningitis and development of communicating hydrocephalus, again without cysts. His incomplete clinical response was initially attributed to noncompliance with medical treatment, but after he worsened despite directly observed TB therapy, multidrug-resistant TB was suspected. His fourth clinical decline included worsening hydrocephalus and discussion of ventriculoperitoneal shunt placement. He was readmitted to the hospital for new diagnostic tests. Empirical therapy was broadened to include antihelminthic treatment. His CSF was submitted for research-based mNGS. The mNGS data indicated no sequences aligning to mycobacterial species. However, 58 789 unique, nonhuman read-pairs aligned to the genus *Taenia* (**Table 2**), with the vast majority specifically mapping to the *T solium* genome (Figure 2). A CSF specimen that had been sent concurrently for fungal 18s ribosomal RNA (rRNA) polymerase chain reaction (PCR) unexpectedly amplified the *T solium* 18s rRNA gene, and the result of a CSF cysticercosis IgG antibody test was positive. A fast imaging protocol employing a steady-state acquisition sequence was included for the first time on the brain MRI, and the results revealed tangled hypointensities in the basilar cisterns, most prominently involving the prepontine cistern with extension into the right side internal auditory canal. After 8 months of antihelminthic treatment, he clinically improved to baseline except for a residual action tremor.

Participant 2 was a 34-year-old woman who had immigrated to the United States from Central America 13 years earlier. She presented with 9 months of right-sided headache, left-sided facial numbness, right-sided pulsatile tinnitus, and recurrent loss of consciousness. Brain MRI showed hydrocephalus and right anterior temporal lobe and prepontine cysts (Figure 3B). Her CSF examination revealed an opening pressure of 36 cm, a WBC count of 115 000/μL comprising 1% neutrophils, 31% monocytes, 46% lymphocytes, 21% plasmacytoid lymphocytes, and 1% eosinophils, a RBC count of 2×10^6/μL, a glucose level of less than 10 mg/dL, and a total protein level of 89 mg/dL. After her CSF and serum cysticercosis IgG antibody test results returned positive, she was treated with albendazole and prednisone for more than 1 month. However, she developed worsening neck pain, and a repeated CSF examination showed elevated intracranial pressure, pleocytosis with a new eosinophilia, an undetectable glucose level, and an elevated total protein level, raising concern for an alternative diagnosis. Her CSF mNGS data contained 569 read-pairs (Table 2) aligning to the genus *Taenia* (Figure 2). She was treated with dual antihelminthic therapy and adjunctive glucocorticoids and had an excellent clinical response.

Cryptococcus neoformans
Participant 3 was a 52-year-old man with a history of migraine and an HIV-1 infection diagnosed in 2013 (viral load detectable but <40 copies/mL; CD4 count 20 cells/μL). He also
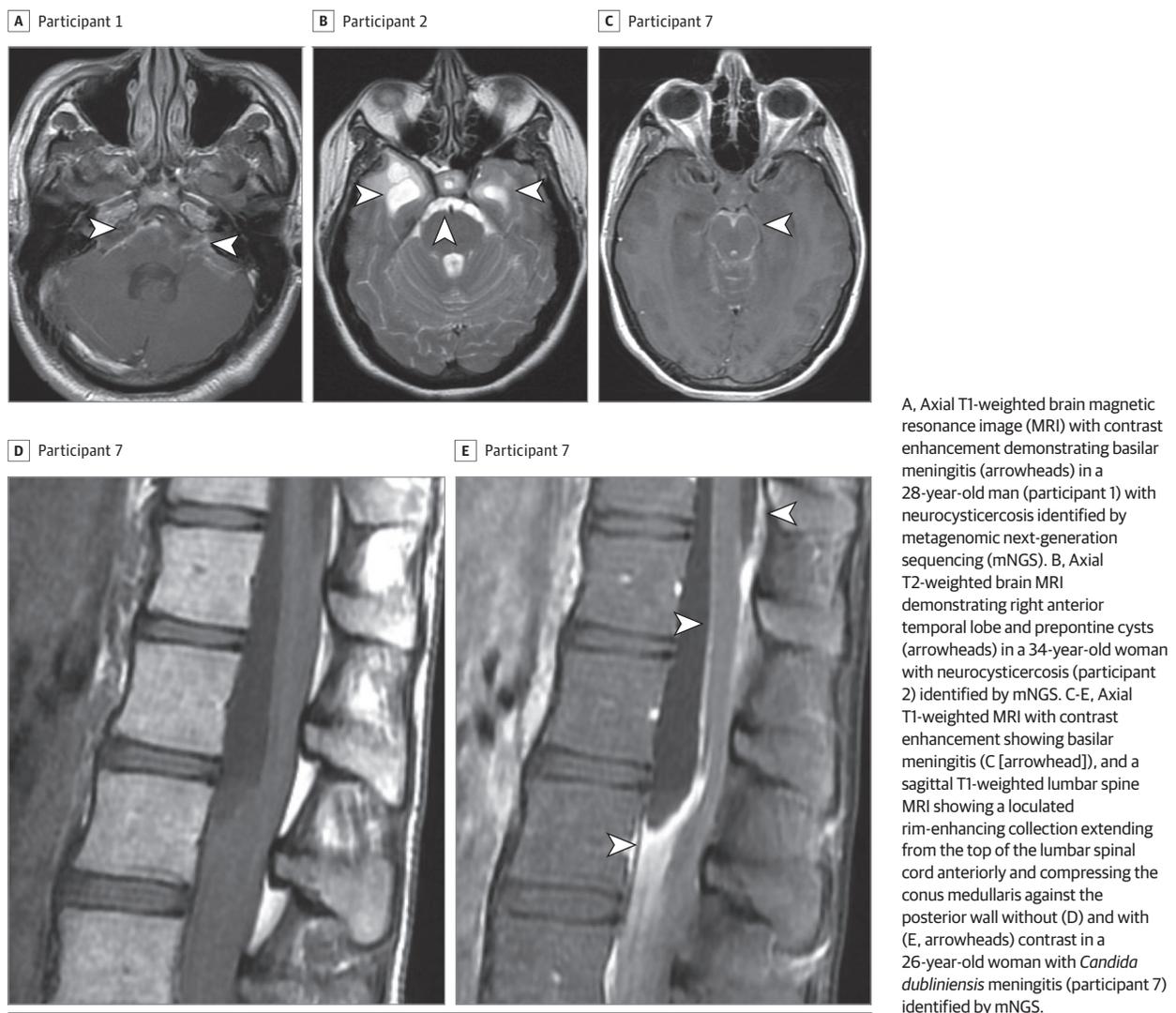
Figure 3. Selected Neuroimaging

A Participant 1   **B** Participant 2   **C** Participant 7

D Participant 7   **E** Participant 7

A, Axial T1-weighted brain magnetic resonance image (MRI) with contrast enhancement demonstrating basilar meningitis (arrowheads) in a 28-year-old man (participant 1) with neurocysticercosis identified by metagenomic next-generation sequencing (mNGS). B, Axial T2-weighted brain MRI demonstrating right anterior temporal lobe and prepontine cysts (arrowheads) in a 34-year-old woman with neurocysticercosis (participant 2) identified by mNGS. C-E, Axial T1-weighted MRI with contrast enhancement showing basilar meningitis (C [arrowhead]), and a sagittal T1-weighted lumbar spine MRI showing a loculated rim-enhancing collection extending from the top of the lumbar spinal cord anteriorly and compressing the conus medullaris against the posterior wall without (D) and with (E, arrowheads) contrast in a 26-year-old woman with *Candida dubliniensis* meningitis (participant 7) identified by mNGS.

Table 2. Metagenomic Sequencing Summary in the 7 Participants

Participant No.	Pathogen	Paired-End Read-Pairs, Total No.	Unique Nonhuman Nonredundant Read-Pairs, No.	Unique Pathogen Read-Pairs, No. (% Nonhuman Read-Pairs)
1	*Taenia solium*	13 141 550	63 435	58 789 (92.7)
2	*T solium*	17 712 171	3732	569 (15.2)
3	*Cryptococcus neoformans*	11 121 312	1678	839 (50.0)
4	HIV-1	8 529 421	261 847	136 000 (51.9)
5	*Aspergillus oryzae*	14 698 597	2753	857 (31.1)
6	*Histoplasma capsulatum*	13 385 787	9406	33 (0.4)
7	*Candida dubliniensis*	14 726 483	7636	68 (0.9)

had a history of injection drug use, hepatitis C virus infection, *Staphylococcus aureus* endocarditis, and syphilis. He presented with agitation, confusion, and ataxia. Because of his prior *S aureus* bacteremia, syphilis, history of migraine, and immunosuppressed state, the differential diagnosis remained broad. Metagenomic next-generation sequencing of his CSF identified 839 unique read-pairs (Table 2) that aligned

to the genus *Cryptococcus* and virtually all aligned to *Cryptococcus neoformans*. Serum cryptococcal antigen test results were positive at a titer greater than 1:160, and CSF cryptococcal antigen test results were positive at a titer greater than 1:1280. Numerous fungal yeast forms were present in the CSF, and *C neoformans* grew in the CSF fungal culture. Except for hepatitis C virus, no other pathogens were identified via CSF

mNGS (Figure 2) or by standard diagnostic assays. He clinically improved on additional treatment with anticryptococcal therapy.

Recurrent Encephalopathy With Known HIV-1 Infection

Participant 4 was a 55-year-old man with a treatment-naive HIV-1 infection that had been diagnosed 8 years earlier. He presented to the emergency department with 2 weeks of confusion and decreased verbal output as well as with several months of cough, intermittent night sweats, and weight loss; his CD4 count was 6 cells/μL. A brain MRI showed bilateral confluent nonenhancing white matter T2 hyperintensities. A CSF examination showed that both his WBC and RBC counts were 0/μL, his glucose level was 34 mg/dL, and his total protein level was 93 mg/dL. Cerebrospinal fluid mNGS testing revealed more than 136 000 unique read-pairs aligning to HIV-1 (Table 2, Figure 2). The full-length HIV-1 genome was assembled using the paired read iterative contig extension assembler, version 1.1.2.[21] The mean total read coverage across the HIV-1 genome was 3991. No reads to JC virus, herpesviruses, or fungal pathogens were observed. His clinical course was consistent with HIV-1 dementia, and no opportunistic CNS infections were identified after extensive testing.

Aspergillus oryzae

Participant 5 was a 32-year-old man who presented to the emergency department with 7 months of episodic dizziness, diplopia, headache, and left facial numbness and weakness. He had a history of injection drug use and hepatitis C virus infection. The results of an HIV-1 test were negative. Brain MRI revealed contrast enhancement in the left pons, middle cerebellar peduncle, and right posterior aspect of the pituitary infundibulum. A computed tomographic angiogram revealed multiple areas of focal stenosis in the posterior circulation. A CSF examination showed a WBC count of 95 000/μL comprising 77% lymphocytes, 13% neutrophils, 6% monocytes, and 4% reactive lymphocytes, a RBC count of 0/μL, total protein level of 61 mg/dL, and a glucose level of 45 mg/dL. Test results for blood and CSF bacterial and fungal cultures were negative. He was treated with glucocorticoids for a suspected autoimmune process. Two weeks later, the patient's symptoms worsened. Repeated brain MRI revealed a new punctate infarct in the right thalamus. Repeated CSF examination showed worsening pleocytosis with a neutrophilic predominance. Bacterial cultures were negative for organisms. Test results for CSF *Aspergillus* galactomannan returned positive at 11.26 (positive, >0.5). The results of a third CSF examination showed an even greater pleocytosis, with a WBC count of 343 000/μL comprising 63% lymphocytes, 20% neutrophils, 15% monocytes, and 2% reactive lymphocytes. Findings for *Aspergillus* galactomannan in the CSF remained elevated at 7.23. Cerebrospinal fluid mNGS returned 857 read-pairs mapping to *Aspergillus* species (Table 2), with the majority of the reads mapping to *Aspergillus oryzae*. The CSF 18s rRNA PCR result was also positive for *Aspergillus* species, and the CSF (1,3) β-D-glucan level was elevated above reference values. No cause of immunocompromise was identified, and no systemic *Aspergillus* infection was identified. Treatment with oral vori-

conazole was initiated, and hydrocephalus was managed with ventriculoperitoneal shunting. The patient was then lost to follow-up.

Histoplasma capsulatum

Participant 6 was a 10-year-old girl with an early childhood spent in the Midwest. She presented in the Northwest with 6 months of back pain and 10 days of progressive left facial droop, headache, neck pain, and vomiting. On examination, she was found to have severe meningismus. Brain and spinal MRI findings were remarkable for diffuse leptomeningeal enhancement. A CSF examination revealed a WBC count of 68 000/μL comprising 33% neutrophils and greater than 30% monocytes, a RBC count of 98×10^6/μL, glucose level less than 20 mg/dL, and total protein level of 292 mg/dL. Empirical therapy was initiated for bacterial meningitis, herpes simplex virus, and endemic mycoses. She developed respiratory failure and paraplegia. Repeated neuroimaging results indicated new pontine infarcts and nonenhancing longitudinal T2 hyperintensities throughout the cervicothoracic cord. Her therapy was broadened to cover TB meningitis. Ultimately, CSF results from fungal culture and 18s rRNA PCR revealed *H capsulatum*. The mNGS data showed 33 read-pairs mapping to *H capsulatum* (Table 2, Figure 2). After 2 months of treatment, she could ambulate but continued to have profound left hearing loss, facial weakness, and neurogenic bladder.

Candida dubliniensis

Participant 7 was a 26-year-old woman with an initially undisclosed history of injection drug use who presented with 1 year of atraumatic lower back pain followed by subacute development of saddle anesthesia and left foot drop. Her MRI results indicated a loculated rim-enhancing collection extending from the top of the lumbar spine anteriorly, compressing the conus medullaris against the posterior wall, in addition to diffuse leptomeningitis involving the entire spinal cord and brainstem (Figure 3C-E). Cisternal CSF showed a WBC count of 126 000/μL comprising 67% neutrophils, 22% lymphocytes, and 11% monocytes, an RBC count of 4×10^6/μL, a total protein level of 105 mg/dL, and a glucose level of 40 mg/dL. Extensive infectious disease diagnostic studies were unrevealing, and 11 weeks later the patient underwent lumbar meningeal biopsy. The pathology findings revealed noninflammatory dense fibrous tissue, and no microbes were identified. Consistent with the pathology results showing no evidence of active infection in the biopsy specimen, 18s rRNA and 16s rRNA PCR tests and mNGS of the biopsy specimen revealed no evidence of infection. In addition, 18s rRNA PCR test results of the CSF were also negative. Three months later, the patient required the use of a wheelchair. Repeated cisternal CSF showed a WBC count of 700 000/μL comprising 81% neutrophils, 16% lymphocytes, 2% monocytes, and 1% eosinophils, a RBC count of 2×10^6/μL, total protein level of 131 mg/dL, and a glucose level of 44 mg/dL. Cerebrospinal fluid mNGS revealed 68 read-pairs mapping to *Candida* species (Table 2), with 61 of the 68 pairs mapping to *Candida dubliniensis* with 99% to

100% identity. The CSF (1,3) β-D-glucan assay result was 211 pg/mL (normal, <80 pg/mL), whereas the serum (1,3) β-D-glucan assay had repeatedly shown normal levels. Findings from repeated CSF 18s rRNA and 16s rRNA PCR assays were negative. The patient was treated with combination antifungal therapy and showed mild clinical improvement, normalization of her CSF profile [including an undetectable CSF (1,3) β-D-glucan level], and decreasing leptomeningeal enhancement on MRI. Of the 3 previously reported patients who have received a diagnosis of *C dubliniensis* meningitis, 2 patients had a history of injection drug use.[27-29]

Reagent and Environmental Contaminant Background Signatures

Examination of nucleotide alignments generated by nontemplated water-only control samples (n = 24) and noninfectious CSF samples (n = 94) revealed 4400 unique bacterial, viral, and eukaryotic genera (eTable in Supplement 1). This microbial background signature was dominated (>70%) by consistent proportions of bacterial taxa, primarily the Proteobacteria and Actinobacteria phyla (eFigure 1 A and B in Supplement 2) representing common soil, skin, and environmental flora previously reported as laboratory and reagent contaminants.[16] To determine if these common microbial contaminants may have been misclassified as pathogens in previously published studies, we examined publicly available data from 2 cases of meningoencephalitis for which a possible infection was identified by mNGS.[19] In each case, neither organism (*Delftia acidovorans* or *Elizabethkingia*) was present at levels significantly greater than the mean of our background data set of water-only and noninfectious CSF control samples (eFigure 1C in Supplement 2). We then examined data from 2 studies aiming to characterize the "brain microbiome" and correlate brain dysbiosis to disease.[17,18] The abundance of the purported brain microbiota revealed distributions that were well within the observed variance of our set of background water-only nontemplated control samples (eFigure 1D in Supplement 2). The authors of the brain microbiome studies[17,18] did not deep sequence water controls when they were unable to generate measurable quantities of DNA after reverse transcription-PCR. The presence of environmental contaminants is due in part to low amounts of input RNA, which is frequently the case with acellular CSF samples, combined with the high number of PCR amplification cycles necessary to generate a sequencing library. To assess this explicitly, we performed an RNA doping experiment (eFigure 2 in Supplement 2) on a water sample and an uninfected CSF sample from which there was no detectable complementary DNA after reverse transcription-PCR. The mNGS library generated from the water had 9.4% unique nonhuman sequences, and that from the CSF sample had 7.6% unique nonhuman sequences. The proportion of nonhuman sequences markedly dropped after spiking with only 20 pg of RNA of a known identity, suggesting that nonhuman environmental sequences are particularly problematic for low input nucleic acid samples, which is often the case for CSF.

Discussion

We presented 7 diagnostically challenging cases of subacute or chronic meningitis in which the use of mNGS of CSF identified a pathogen, including a case of subarachnoid neurocysticercosis that had defied diagnosis for 1 year, the first reported case of CNS vasculitis caused by *A oryzae*, and the fourth reported case of *C dubliniensis* meningitis. A straightforward statistical model leveraging a large mNGS data set obtained from water-only nontemplated control samples and from patients with a variety of noninfectious neuroinflammatory syndromes correctly prioritized the pathogens. Larger prospective studies are needed to determine the clinical utility of this approach for reducing the number of false-positives and false-negatives.

The use of CSF mNGS has the potential to overcome several limitations of conventional CNS infectious disease diagnostics. First, the inherent risks of brain or meningeal biopsy make CSF mNGS a particularly attractive and less invasive diagnostic option for patients with suspected CNS infection. Second, the large number of neuroinvasive pathogens that cause subacute or chronic meningitis makes it logistically challenging and cost prohibitive to order every possible neuroinfectious diagnostic test using a candidate-based approach. Third, some assays lack sensitivity in the context of impaired immunity or acute infection (eg, West Nile virus serology), can be slow to yield results (eg, mycobacterial and fungal cultures), or may fail to differentiate between active infection and prior exposure (eg, cysticercosis antibody or interferon-gamma release assay for TB).

The unbiased nature of mNGS makes the data sets inherently polymicrobial and complex. Thus, statistical scoring and filtering is essential to enhance the ability to discriminate between insignificant contaminants and true infectious organisms. Our algorithm correctly prioritized etiologic pathogens among these 7 clinically confirmed cases of infectious meningitis despite the pathogens ranging widely in absolute abundance (33-136 000 sequence read-pairs) and in the proportion of the nonhuman sequences (0.9%-92.7%) that they comprised (Table 2).

We also analyzed a recently published clinical mNGS data set[19] to highlight that a thorough profile of the microbes present in water-only control and noninfectious CSF samples reinforces the skepticism with which those authors described a possible infection of 1 participant with *Delftia acidovorans* (patient 2) and of another participant with *Elizabethkingia* (patient 7) (eFigure 1C in Supplement 2). Furthermore, such a database could help improve the accuracy of microbiome studies, especially for body sites historically considered sterile in which rigorous controls are necessary to establish that observed microbial sequences represent microbiota vs environmental contaminants (eFigure 1D in Supplement 2).[18,19] This problem appears to be particularly critical in samples, such as those from the CSF, in which subnanogram levels of input RNA or DNA require unbiased molecular amplification steps before sufficient material is available for sequencing applications. Indeed, the addition of only 20 pg of purified RNA to a CSF sample was sufficient to suppress the majority of nonhuman reads derived from the water and reagents (eFigure 2 in Supplement 2). Although amplifying the input signal increases the sensi-

tivity of the assay, it also often overrepresents the signature of contaminating taxa unique to a given laboratory, experimenter, or reagent lot.[14,16] These results provide a cautionary note and underscore the need for appropriate controls to aid in interpretation.

Limitations

We expect that larger databases of patient mNGS results will only enhance the ability to discriminate between irrelevant sequences and legitimate pathogens and permit more rigorous and probabilistic models for pathogen ranking and reporting. We presented herein 1 empirically derived system for prioritizing results based on the read count weighted by standard z scores. Given the sensitivity of NGS-based approaches, we anticipate that individual laboratories will need to develop their own dynamic reference data sets to control for contaminants that are relevant to the particular time, place, and manner in which the biological samples are being analyzed.

Conclusions

Metagenomic next-generation sequencing represents an increasingly rapid and comparatively low-cost means of screening CSF in an unbiased manner for a broad range of human pathogens using a single diagnostic test. Although the present selected case series is not appropriate to measure the performance characteristics in a prospective cohort, a recently completed demonstration project sponsored by the state of California[30] may also prove to be helpful in supporting the exclusion of CNS infection when a coinfection is suspected in an immunosuppressed patient (as illustrated with *C neoformans* and HIV-1) or when a noninfectious cause, such as an autoimmune condition, is clinically favored. On this basis, we foresee the eventual replacement of many single-agent assays performed in reference laboratories with a unified mNGS approach.

REFERENCES

1. Zunt JR, Baldwin KJ. Chronic and subacute meningitis. *Continuum (Minneap Minn).* 2012;18(6 Infectious Disease):1290-1318.

2. Baldwin KJ, Zunt JR. Evaluation and treatment of chronic meningitis. *Neurohospitalist*. 2014;4(4): 185-195.

3. Wilson MR, Naccache SN, Samayoa E, et al. Actionable diagnosis of neuroleptospirosis by next-generation sequencing. *N Engl J Med*. 2014; 370(25):2408-2417.

4. Wilson MR, Shanbhag NM, Reid MJ, et al. Diagnosing *Balamuthia mandrillaris* encephalitis with metagenomic deep sequencing. *Ann Neurol*. 2015;78(5):722-730.

5. Wilson MR, Zimmermann LL, Crawford ED, et al. Acute West Nile virus meningoencephalitis diagnosed via metagenomic deep sequencing of cerebrospinal fluid in a renal transplant patient. *Am J Transplant*. 2017;17(3):803-808.

6. Murkey JA, Chew KW, Carlson M, et al. Hepatitis E virus-associated meningoencephalitis in a lung transplant recipient diagnosed by clinical metagenomic sequencing. *Open Forum Infect Dis*. 2017;4(3):ofx121.

7. Wilson MR, Suan D, Duggins A, et al. A novel cause of chronic viral meningoencephalitis: Cache Valley virus. *Ann Neurol*. 2017;82(1):105-114.

8. Naccache SN, Peggs KS, Mattes FM, et al. Diagnosis of neuroinvasive astrovirus infection in an immunocompromised adult with encephalitis by unbiased next-generation sequencing. *Clin Infect Dis*. 2015;60(6):919-923.

9. Palacios G, Druce J, Du L, et al. A new arenavirus in a cluster of fatal transplant-associated diseases. *N Engl J Med*. 2008;358(10):991-998.

10. Quan PL, Wagner TA, Briese T, et al. Astrovirus encephalitis in boy with X-linked agammaglobu-linemia. *Emerg Infect Dis*. 2010;16(6):918-925.

11. Flygare S, Simmon K, Miller C, et al. Taxonomer: an interactive metagenomics analysis portal for universal pathogen detection and host mRNA expression profiling. *Genome Biol*. 2016;17(1):111.

12. Naccache SN, Federman S, Veeraraghavan N, et al. A cloud-compatible bioinformatics pipeline for ultrarapid pathogen identification from next-generation sequencing of clinical samples. *Genome Res*. 2014;24(7):1180-1192.

13. Wood DE, Salzberg SL. Kraken: ultrafast metagenomic sequence classification using exact alignments. *Genome Biol*. 2014;15(3):R46.

14. Naccache SN, Greninger AL, Lee D, et al. The perils of pathogen discovery: origin of a novel parvovirus-like hybrid genome traced to nucleic acid extraction spin columns. *J Virol*. 2013;87(22): 11966-11977.

15. Lee D, Das Gupta J, Gaughan C, et al. In-depth investigation of archival and prospectively collected samples reveals no evidence for XMRV infection in prostate cancer. *PLoS One*. 2012;7(9):e44954.

16. Salter SJ, Cox MJ, Turek EM, et al. Reagent and laboratory contamination can critically impact sequence-based microbiome analyses. *BMC Biol*. 2014;12:87.

17. Branton WG, Ellestad KK, Maingat F, et al. Brain microbial populations in HIV/AIDS: α-proteobacteria predominate independent of host immune status. *PLoS One*. 2013;8(1):e54673.

18. Branton WG, Lu JQ, Surette MG, et al. Brain microbiota disruption within inflammatory demyelinating lesions in multiple sclerosis. *Sci Rep*. 2016;6:37344.

19. Salzberg SL, Breitwieser FP, Kumar A, et al. Next-generation sequencing in neuropathologic diagnosis of infections of the nervous system. *Neurol Neuroimmunol Neuroinflamm*. 2016;3(4):e251.

20. Dobin A, Davis CA, Schlesinger F, et al. STAR: ultrafast universal RNA-seq aligner. *Bioinformatics*. 2013;29(1):15-21.

21. Ruby JG, Bellare P, DeRisi JL. PRICE: software for the targeted assembly of components of (Meta) genomic sequence data. *G3 (Bethesda)*. 2013;3(5): 865-880.

22. Fu L, Niu B, Zhu Z, Wu S, Li W. CD-HIT: accelerated for clustering the next-generation sequencing data. *Bioinformatics*. 2012;28(23):3150-3152.

23. Ziv J, Lempel A. A universal algorithm for sequential data compression. *IEEE Trans Inf Theory*. 1977;23(3):337-343. doi:10.1109/TIT.1977.1055714

24. Langmead B, Salzberg SL. Fast gapped-read alignment with Bowtie 2. *Nat Methods*. 2012;9(4): 357-359.

25. Wu TD, Nacu S. Fast and SNP-tolerant detection of complex variants and splicing in short reads. *Bioinformatics*. 2010;26(7):873-881.

26. Zhao Y, Tang H, Ye Y. RAPSearch2: a fast and memory-efficient protein similarity search tool for next-generation sequencing data. *Bioinformatics*. 2012;28(1):125-126.

27. van Hal SJ, Stark D, Harkness J, Marriott D. *Candida dubliniensis* meningitis as delayed sequela of treated *C. dubliniensis* fungemia. *Emerg Infect Dis*. 2008;14(2):327-329.

28. Andrew NH, Ruberu RP, Gabb G. The first documented case of *Candida dubliniensis* leptomeningeal disease in an immunocompetent host. *BMJ Case Rep*. 2011;2011:bcr0620114384.

29. Yamahiro A, Lau KH, Peaper DR, Villanueva M. Meningitis caused by *Candida dubliniensis* in a patient with cirrhosis: a case report and review of the literature. *Mycopathologia*. 2016;181(7-8):589-593.

30. California Initiative to Advance Precision Medicine. Precision Diagnosis of Acute Infectious Diseases. http://www.ciapm.org/project/precision-diagnosis-acute-infectious-diseases. Published 2016. Accessed February 28, 2018.